Journal of Optoelectronics and Advanced Materials Vol. 5, No. 5, 2003, p. 1381 - 1387

MICROSTRIP PATCH ANTENNA WITH DIELECTRIC SUBSTRATE

D. D. Sandu*, O. Avadanei, A. Ioachim[a], G. Banciu[a], P. Gasner

"Al. I. Cuza" University of Iaşi
[a]INFIM Bucharest

The paper refers to the study of patch antennas with a high permittivity dielectric substrate ($(Zr_{0.8}\ Sn_{0.2})TiO_4$) obtained at National Institute of Materials Physics Bucharest. Because of the high value of the permittivity of the substrate material it was necessary to perform a comparative investigation of different prototypes and arrays. It was considered two substrate thickness h_1=1mm and h_2=2mm and two frequencies f_1=2.4 GHz and f_2=1.8 GHz. For each case we presented the radiation pattern in the two principal planes (E and H) and input impedance. Also, some radiation pattern for rectangular array with n=4, 16, 36 patches are presented. In the Conclusion section a discussion on the suitability of patch antennas with high permittivity substrate is done.

(Received July 10, 2003; accepted August 28, 2003)

Keywords: High permittivity dielectrics, Patch antennas, Input impedance, Radiation pattern, Antenna array

1. Introduction

Generally, the advantages and drawbacks of patch antennas with high permittivity substrate is a controversial problem and some interesting results are reported in [1] [2] [3]. In this paper we performed an investigation on patch antennas built on a high permittivity substrate. The ZST dielectric is made at National Institute of Material Physics. This material was synthesized by conventional solid-state methods from individual high-purity oxide powders (>99.9%). The starting materials were mixed according to the desired stoechiometry of $(Zr_{0.8}, Sn_{0.2})TiO_4$ ceramics, with a 2 wt % La_2O_3 and 1 wt % ZnO additions as a sintering aid. The powders were ground in distilled water for 24h in a mill with agate balls. All the mixtures were dried and treated at 1200 ^oC for 2h. The calcined powders with 0.2 wt% NiO addition were then remilled for 2h with PVA solution as a binder. Substrate plates were formed by uniaxial pressing and sintered at temperatures of (1330-1400) ^oC for (2-4)h.

The morphology, phase-composition and microstructure observation of the sintered ceramics was performed by means of scanning electron microscopy (SEM), and energy-disperse X-ray spectrometry (EDX). The crystalline phases were identified by X-ray diffraction (XRD) patterns.

The dielectric permittivity (ε_r) and the quality factor values (Q) at microwave frequencies were measured using the Hakki-Coleman dielectric resonator method.

The basic relations refer to the radiation patterns of patches and to the input impedances. The rectangular patch and the coordinate system for the cavity are shown in Fig. 1a. In order to establish some important relation concerning the radiation pattern of a patch a simple model was adopted: the field $\vec{E}$ has only z component whereas the field $\vec{H}$ has only xy component only; both $\vec{E}$ and $\vec{H}$ are independent are independent of z coordinate for all the frequencies of interest; the tangent component of the $\vec{H}$ along the edge has a negligible value, therefore the electric current has no component perpendicular to the edge. This simple model can be applied for patch antennas because they have a very small dimension along the z axis.

* Corresponding author: ddsandu@uaic.ro

The region between patch and ground plane can be treated as a cavity bounded by magnetic walls along the edge and by electric walls on the top and bottom. If such a cavity is excited by a microstrip line or by a coaxial line Fig. 2 the field inside cavity represent a superposition of all TM_{mn0} modes; the z-directed component of $\vec{E}$ can be assumed as [4,5]:

$$E_z(x,y) = \sum_m \sum_n A_{mn}\, \vec{e}_{mn}(x,y) \tag{1}$$

where A_{mn} are the mode amplitude coefficient and $\vec{e}_{mn}$ are the z-directed orthonormalized electric field mode vector.

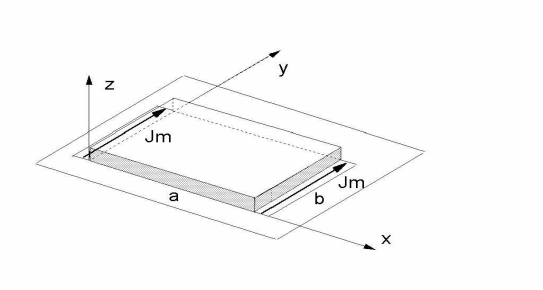

Fig. 1a.

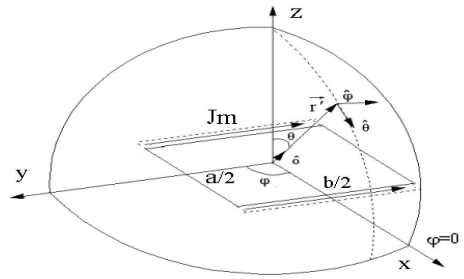

Fig. 1b.

For a nonradiating cavity the E_z component has the following form:

$$E_z = E_0 \cos k_m x \cos k_m y \cos k_p z \tag{2}$$

and the x,y components of magnetic fields are:

$$H_x = \frac{j\omega_r \varepsilon}{k_{mnp}^2} k_y E_0 \cos k_m x \sin k_n y \cos k_p z$$

$$H_y = \frac{j\omega_r \varepsilon}{k_{mnp}^2} k_x E_0 \sin k_m x \cos k_n y \cos k_p z \tag{3}$$

where: $k_{mnp}^2 = k_m^2 + k_n^2 + k_p^2$, and $k_m = m\pi/a \quad k_n = n\pi/b \quad k_p = p\pi/t$; ω_r is the resonant frequency. Usually a dominant mode of oscillation is assumed; such a mode is TM_{100} described by the relations:

$$E_z = E_0 \cos \pi x/a \tag{4}$$

$$H_y = jH_0 \sin \pi x/a \tag{5}$$

where $H_0=E_0/Z$ and $Z = (\mu_0/\varepsilon_r)^{1/2}$.

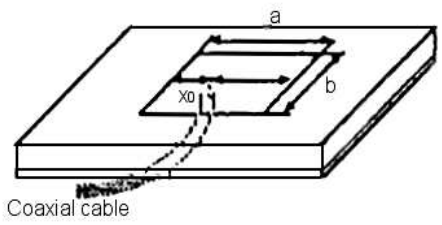

Fig. 2a. Coaxial feed patch.

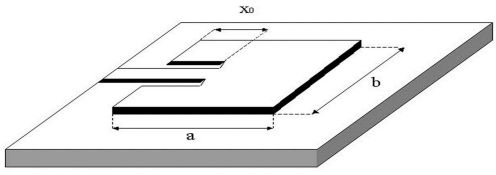

Fig. 2b. Microstrip line feed patch.

In the case of radiating microstrip patches (real cavity) the eigenvalues became complex quantities and $|k_m|, |k_n|$ are slightly less then $m\pi/a$ and $n\pi/b$.

For the dominant mode TM_{100} we have only magnetic currents on the edge, defined by general relation $\vec{J}_{ms} = -\hat{n} \times \vec{E}_a$ where $\vec{E}_a$ is the electric field in the aperture at the edge and $\hat{n}$ is the outgoing unit vector from the edge. It is shown that only the currents [6]:

$$\vec{J}_{ms1}(x=0) = -2\hat{n} \times \vec{E}_a = \hat{j}2E_z(x,y)$$
$$\vec{J}_{ms2}(x=a) = -2\hat{n} \times \vec{E}_a = \hat{j}2E_z(x,y) \tag{6}$$

are radiating in the free space.

In order to analyze the radiating properties of the microstrip patch antennas we will assume the coordinate system shown in Fig. 1b, in witch the coordinate origin coincide with the symmetry center of the antenna. The radiated fields in the Fraunhofer zone have the expressions [7]:

$$E_\theta = -\frac{jk}{\pi r}\exp(-jk_0 r)E_0 \cdot \int_0^t \int_{-b/2}^{b/2} e^{(jk_0 y \sin\theta \sin\varphi)} \left(e^{(-\frac{jk_0 a \sin\theta\cos\varphi}{2}} + e^{(\frac{jk_0 a \sin\theta\cos\varphi}{2}} \right) dydt \cos\varphi \cdot \tag{7}$$

$$E_\varphi = -\frac{jk}{\pi r}\exp(-jk_0 r)E_0 \cdot \int_0^t \int_{-b/2}^{b/2} e^{(jk_0 y \sin\theta \sin\varphi)} \left(e^{(-\frac{jk_0 a \sin\theta\cos\varphi}{2}} + e^{(\frac{jk_0 a \sin\theta\cos\varphi}{2}} \right) dydt \sin\varphi\cos\theta \cdot$$

From these relations we can determine the radiated fields until a constant E_0 that depends of the excitation.

The input impedance of a patch antenna is of great practical importance because if the patch is not adapted to the feed line the antenna would not radiate at all. The input impedance is calculated by the relation[8,9]:

$$\frac{1}{R_{mn}} = \frac{\mu_0 hc^2}{\varepsilon_r \omega_{mn} \delta_{eff}} \psi_{mn}^2(x_0, y_0) G_{mn} \tag{8}$$

where $G_{mn} = \frac{\sin(n\pi d_x/2a)}{n\pi d_x/2a} \cdot \frac{\sin(m\pi d_y/2b)}{m\pi d_y/2b}$ and $\psi_{mn} = \frac{\chi_{mn}}{\sqrt{ab}} \cos k_n x \cos k_m y$

The factor G_{mn} accounts for the width of the feed, c is the speed of light, δ_{eff} is an effective loss tangent in witch are included also the losses in metallic walls and the radiating losses, and χ_{mn} is a normation factor. For microstrip feed patch antennas the effective feed dimensions (d_x, d_y) are taken equals to the physical dimensions of the microstrip line.

The radiation pattern for array antennas is found by multiplying the array factor with the radiating pattern of one element. The array factor for planar array with m elements on x-coordinate and n elements on y-coordinate is given by [6]:

$$E = E_0 \sum_{s=1}^{m} \exp\left(j(s-1)(\delta + kdx \sin\theta\cos\varphi)\right) \sum_{s=1}^{n} \exp\left(j(s-1)(\delta + kdy \sin\theta\sin\varphi)\right)$$

where δ is the phase factor between two consecutive elements and dx, dy are the distances between two consecutive elements along the x respective y axes; E_0 is the field radiated by a patch.

2. Computeted results

We have designed two types of patch antennas, for f_1=1.8 GHz and two types for f_2=2.4 GHz. For the frequency f_1 we considered two substrate thicks h_1=2 mm, h_2=1 mm with the geometrical dimensions for the patchs a_1=14.3 mm, b_1=9.5 mm, a_2=14.4 mm, b_2=9.8 mm. Also for the frequency f_2 we considered the same substrate thick and the dimensions are a_3=10.3 mm, b_3=8.8 mm, a_4=10.7 mm, b_4=8 mm.

The radiation patterns for the 1.8 GHz antennas in the φ=0 plane and φ=90^0 are shown in Fig. 3a and Fig. 3b. In Fig. 4a and Fig.4b we presented the radiation patterns for the 2.4 GHz in the φ=0 plane and respective φ = 90^0 plane. All the radiation patterns are normalized.

We have also presented the dependence of the input impedance with the position of the feeding point for the 1.8GHz antennas in Fig. 5a and for the 2.4 GHz antennas in Fig. 5b. We have calculated the positions of the feed point (Fig. 2) with the best adaptation at the microstrip feed line for the four antennas and the results are: x_{o1}=6.6 mm, x_{o2}=6.4 mm. x_{o3} = 4.7 mm and x_{o4} = 4.8 mm.

Also the radiation patterns for some array antennas were calculated. In Fig. 6 we present the radiation pattern for 1.8 GHz arrays with 4, 16, and 36 elements in the φ=0 plane and for λ/2 distance between elements.

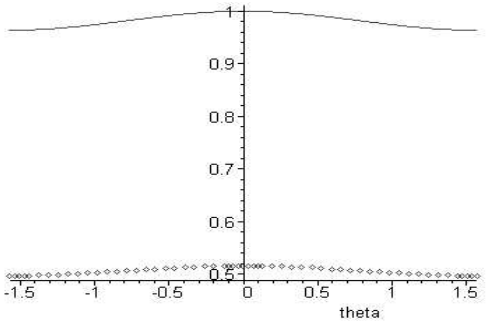

Fig. 3a.

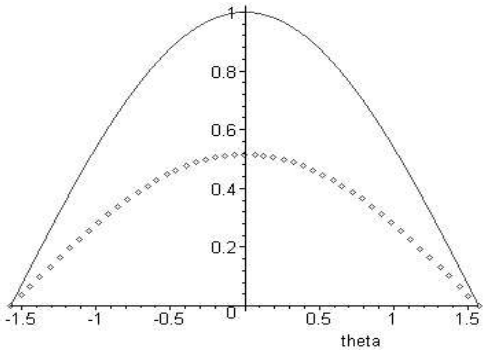

Fig. 3b.

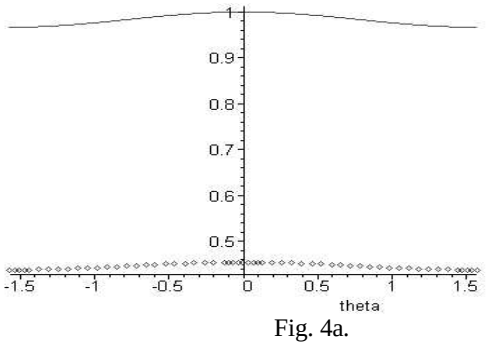

Fig. 4a.

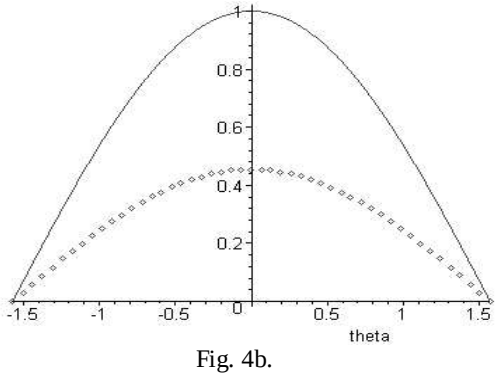

Fig. 4b.

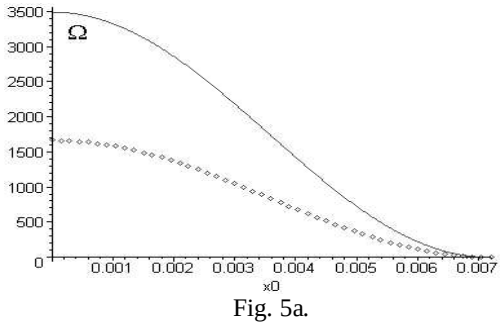

Fig. 5a.

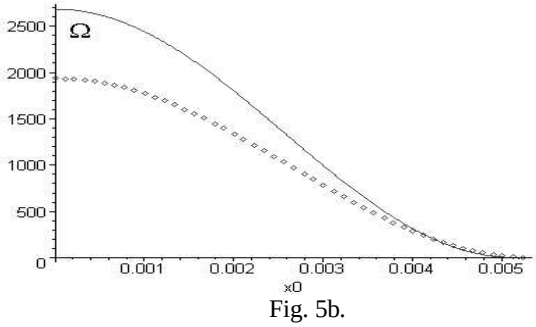

Fig. 5b.

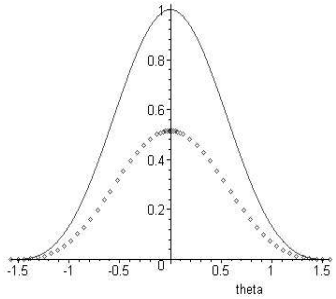

Fig. 6a.

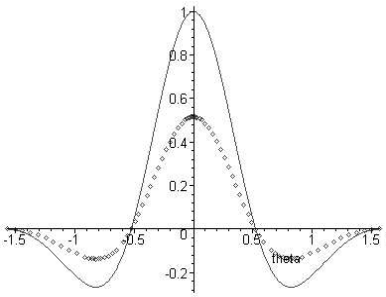

Fig. 6b.

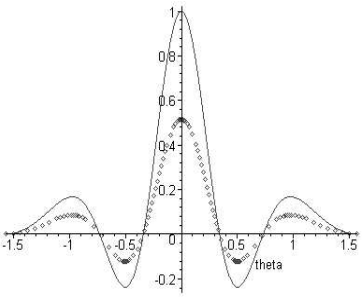

Fig. 6c.

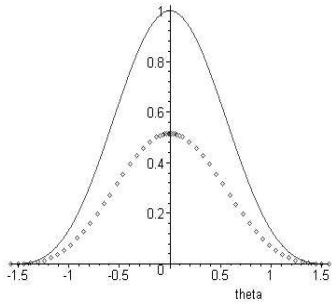

Fig. 7a.

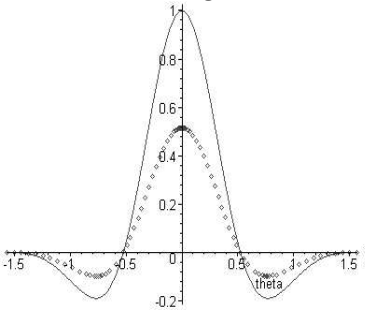

Fig. 7b.

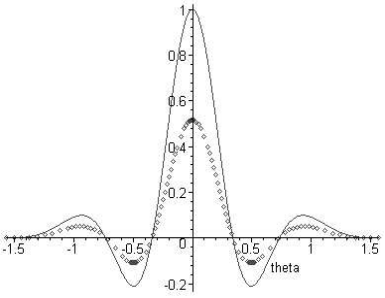

Fig. 7c.

In Fig. 7 we present the radiation pattern for 1.8 GHz arrays with 4, 16, and 36 elements in the $\varphi=90^0$ plane and for $\lambda/2$ distance between elements. In Fig.8 we present the radiation pattern for 1.8 GHz arrays with 4, 16, and 36 elements in the $\varphi=0$ plane and for $\lambda/4$ distance between elements.

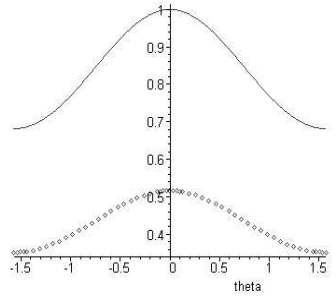

Fig. 8a.

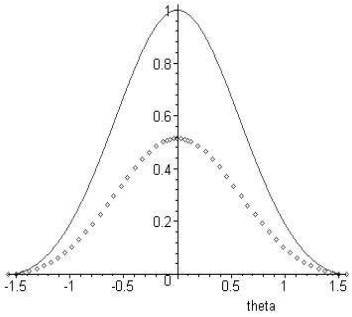

Fig. 8b.

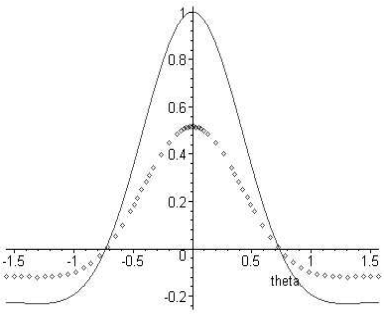

Fig. 8c.

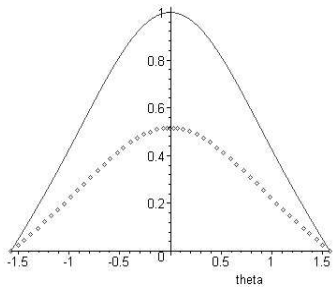

Fig. 9a.

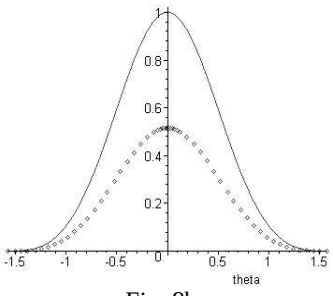

Fig. 9b.

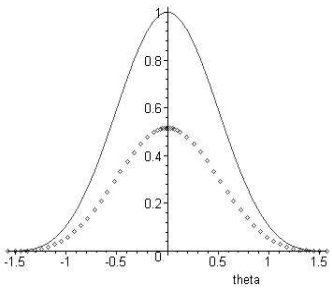

Fig. 9c.

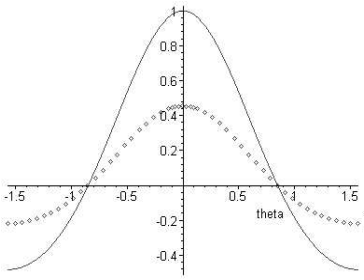

Fig. 10a.

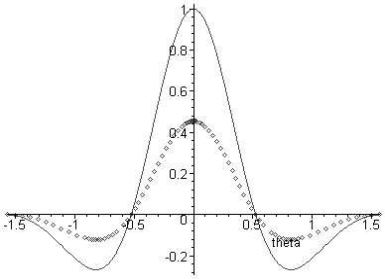

Fig. 10b.

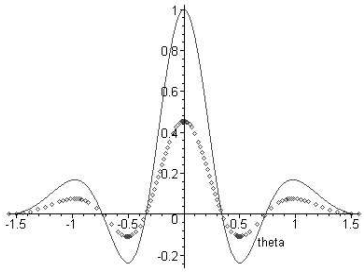

Fig. 10c.

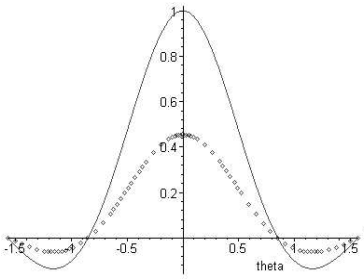

Fig. 11a.

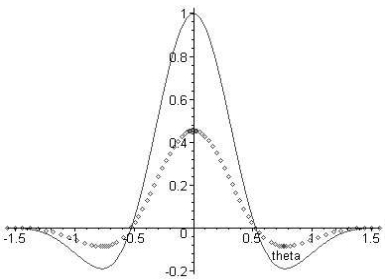

Fig. 11b.

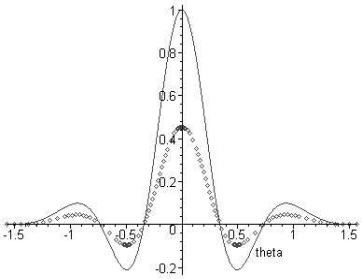

Fig. 11c.

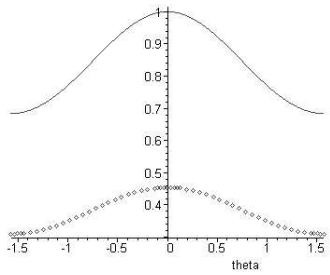

Fig. 12a.

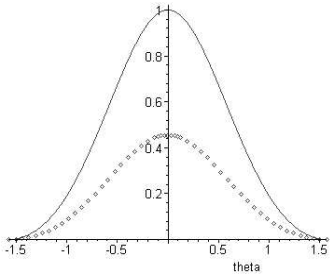

Fig. 12b.

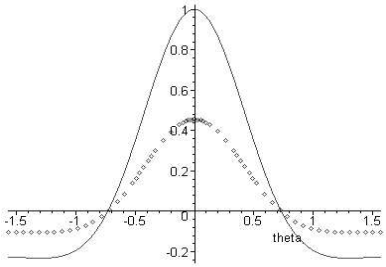

Fig. 12c.

In Fig. 9 we present the radiation pattern for 1.8 GHz arrays with 4, 16, and 36 elements in the $\varphi = 90^0$ plane and for $\lambda/4$ distance between elements. The Figs. 10, 11, 12, and 13 are the correspondent to the Figs. 6, 7, 8 and respective 9 for the 2.4 GHz arrays. For all figures the pointed line is for antennas made on 1mm thickness substrate, and the continuous line is for 2 mm thickness.

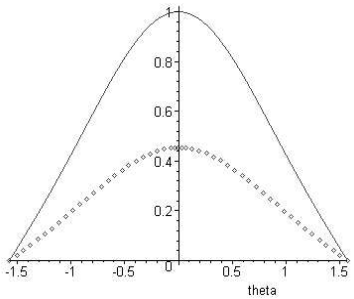

Fig. 13a.

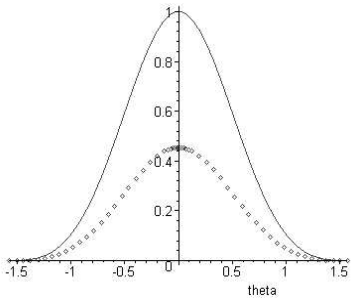

Fig. 13b.

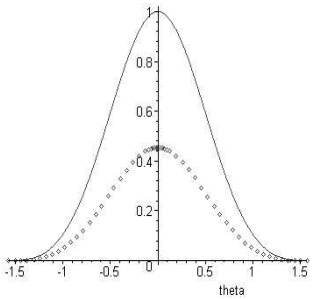

Fig. 13c.

3. Conclusion

The $(Zr_{0.8}, Sn_{0.2})TiO_4$ ceramic has a very high hardness witch make it very difficult to perforate without fracturing the material. For this reason without an ultrasonic perforator the microstrip feed method is the only practical solution.

The length a of the patch antennas determine the radiation frequency, and the breadth *b* have also a small influence to the radiation frequency, to the input impedance and to the radiated power. We have chosen the breadth b to obtain an convenient position of the feed point.

From Fig. 3 and Fig. 4 we can see that the patch antennas have a wide radiation pattern and that the antennas with 2 mm thickness have a significant grater output power, and so are more efficient than the antennas with 1mm substrate thickness. Also the microstip feed line for 2 mm thick antennas are significant wider $w_1 = 0.47$ mm instead for the 1mm thick antennas where $w_2 = 0.17$ mm, and so much easier to manufacture. The only drawback of the 2 mm thick antennas is that the input impedance has a much important variation with the feed point position as we can see from Fig.5. For example for 1.8 GHz antenna with h_1=2mm we have the following real impedances: for $x_{01} = 6.5$ mm, R = 70.72 Ω, for $x_{01} = 6.6$ mm, R = 50.7 Ω, and for $x_{01} = 6.7$ mm, R=34 Ω. In the same time for the 1.8 GHz 1 mm thick antenna we have: for $x_{02} = 6.3$ mm, R = 63 Ω, for $x_{02} = 6.4$ mm, R = 50.16 Ω, and for $x_{02} = 6.5$ mm, R = 38.5 Ω.

For arrays antennas the total power radiated and the intensity of the main lobe depend on the element number. For arrays with λ/2 distance between elements, the directivity increases with the number of element but for arrays with λ/4 distance the directivity is worst and it increases slower with the number of elements. The directivity depends only on the array dimensions.

References

[1] T. K. Lo, Electronic Letters **33**, 9 (1997).
[2] J. S. Colburn, Y. Rahmat-Samii, IEEE Antennas. Propag. **47**(12), 1785 (1999).
[3] Sung-Hun Sim, Chong-Yun Kang, Ji-Won Choi, Seok-Jin Yoon, Hyun-Jai Kim, Young-Joong Yoon, Journal of Materials Science: Materials in electronics **13**, 207 (2002).
[4] Y. T. Lo, D. Solomon, W. F. Richards, IEEE Trans. Antennas Propagation AP-**27**, 137 (1979).
[5] K. R. Carver, J. W. Mink, IEEE Trans. Antennas Propagation **AP-29**, 2 (1981).
[6] N. Balanis, John Wiley and Sons, New York 1989.
[7] A. Ishimaru, Prentice Hall International Edition 1990.
[8] O. G. Avădănei, D. D. Sandu, D. Ionesi, Proc. SCS (IEEE Chapter) Volume 37 (2001),
[9] W. F. Richards, Y. T. Lo, D. Harrison, A.P-**29**, 38 (1981).